Deblending OBC data with dual and triple simultaneous sources offshore Trinidad

Dongping Zhuang, Guangfu Shao, Adel Khalil (CGG); Bertram Nolte, Pedro Paramo, Kareem Vincent (BP)*

Summary

Deblending shallow water OBC data can be challenging. High blending fold, strong early arrivals, shear wave energy in Vz component, and background noise all add to the complexity of the problem. Using an offshore Trinidad OBC survey, including dual and triple sources, we demonstrate the effectiveness of a specialized deblending strategy designed to tackle these challenges. This strategy combines the merits of two deblending techniques: cross-talk modeling and subtraction, and impulsive denoising. The process is guided by a blending-noise level map deterministically derived from actual shooting times. Test results on both P and Vz components confirm the effectiveness of this approach and raise the confidence level of the quality of deblended data.

Introduction

Simultaneous shooting allows for temporal overlap between different sources. This reduces shot-time intervals and thus increases source productivity. Based on survey requirements, survey duration can be reduced, or more shots can be acquired for higher resolution sampling.

Due to the overlap between shots, energy from different records interfere with each other. This cross-talk, or blending interference, requires shot separation prior to traditional processing. The separation process is often referred to as deblending. Deblending techniques have progressed over the years, starting from the early passive approach, where no explicit action is taken on the prestack data and cross-talk attenuation relies on migration stacking power, to the more recent active approaches utilizing different transforms and operations before migration to reduce blending noise (e.g., Abma et al., 2010; Peng and Meng, 2016; Rohnke and Poole, 2016). Several field trials and simulations have established that simultaneous shooting, together with appropriate deblending, can produce images of similar quality as those produced by conventional acquisition (Alexander et al., 2013).

Modeling and impulsive denoising have been two major classes of active deblending techniques. Employing one of them or combining both for deblending has been effective on many data sets. However, shallow water OBC surveys, with very strong and often aliased early arrivals and shear wave energy, pose further challenges to the traditional approaches. Blending noise from these events can arrive later in the record, interfering with weaker events. Its magnitude can be significantly larger than that of background signal. Given the complexity of these wave phenomena and their typical aliased sampling, modeling-based deblending approaches usually underperform. Relatively small cross-talk residual left by the modeling-based method can still completely overwhelm the true signal. Exchanging or complementing modeling-based deblending techniques with brute force impulsive denoising is likely to fail due to its unselective nature. At locations where noise-to-signal ratio is high or when the wavefield is overly complex, signal preservation becomes more difficult.

These challenges are highlighted in a shallow water OBC survey from offshore Trinidad. To address these challenges, we designed and deployed a hybrid deblending methodology. This method operates iteratively by combining modeling-based deblending techniques and a refined impulsive denoise tactic. This refined denoise tactic is guided by shooting times and operates only on the residual from the modeling stage. The modeling aspect of the method ensures signal is preserved as much as possible, while the refined impulsive denoise portion prevents noise from overwhelming true signal in a signal-preserving manner. We demonstrate the results on both P and Vz components acquired by dual and triple sources.

Method

Simultaneous shooting data, $\mathbf{d}$, contain responses of more than one source in the same record. The deblending process recovers an individual source response, $\mathbf{s}$, by separating out blending noise, $\mathbf{n}$. The noise is related to the signal by an alignment operator, $\mathbf{L}$:

$$\mathbf{d} = \mathbf{s} + \mathbf{n} = \mathbf{s} + \mathbf{Ls}, \qquad (1)$$

and the deblending problem is to solve this equation for $\mathbf{s}$. The problem is underdetermined and prior information is required. Randomized shooting times make blending noise incoherent in some domains, e.g., common receiver. This can be utilized to model the signal in the record and is the basis of many deblending techniques. The modeling-based deblending scheme is achieved by predicting signal using a modeling operator, $\mathbf{F}$. A noise model is generated by alignment of the signal model, and the residual is calculated by subtracting the noise model from the data. The whole process is iterated until convergence:

$$\mathbf{s}_{i+1} = \mathbf{s}_i + \mathbf{F}_i\mathbf{r}_i\ ,\ \mathbf{n}_i = \mathbf{Ls}_i\ ,\ \mathbf{r}_i = \mathbf{d} - (\mathbf{s}_i + \mathbf{n}_i)\,. \qquad (2)$$

Different choices exist for the modeling operator, $\mathbf{F}$. We tested several methods on the data and found that f-x projection filtering (Soubaras, 1995) and low-rank decomposition (Sternfels et al., 2015; Wang et al., 2016)

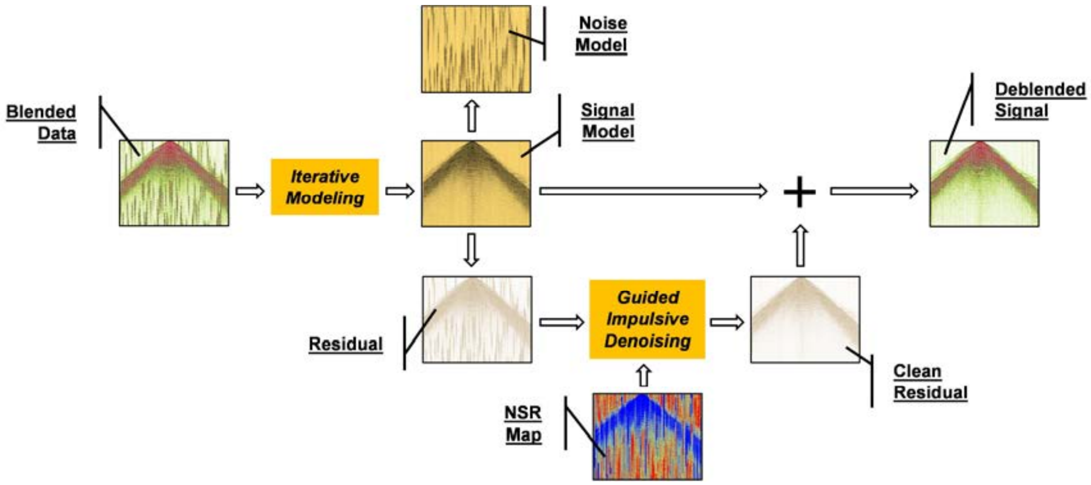

Figure 1. Hybrid deblending algorithm outline.

both worked well. In our implementation, we used f-x filtering because of its speed and flexibility. For shallow water OBC data, cross-talk energy is generally too complex to be fully captured by modeling operators. We complement the deblending process with a deterministic impulsive denoise operation that operates only on the residual.

By synthetically blending the envelope of the estimated signal using the shooting times and comparing to the unblended envelope, a map that identifies the blending-noise level in different areas of the record is created. This map is referred to as the noise-to-signal ratio (NSR) map:

$$M = \mathbf{L}H(\mathbf{s})/H(\mathbf{s})\,. \tag{3}$$

Where $H(\mathbf{s})$ and $\mathbf{L}H(\mathbf{s})$ are the unblended and blended signal envelopes, respectively, and M is the NSR map. Guided impulsive denoising can then be applied to the residual using the map and added to the signal from the modeling phase. Figure 1 illustrates the two-step procedure of this algorithm.

Offshore Trinidad OBC data set

The OBC data set contains two surveys acquired over the Angelin field in the shallow water area, east of Trinidad. Water depth ranges from 50 m to 70 m. Two boats were deployed for each survey using BP's Independent Simultaneous Source (ISS®) technology (Howe et al., 2008; Abma and Keggin, 2012; Abma et al., 2012). Both surveys shared the same receiver cables and had a nominal shot grid of 50 m x 50 m. The first survey had two source arrays on each boat firing approximately every 25 m in a flip-flop configuration. We refer to this survey as the dual-source survey. The second survey, referred to as the triple-source survey, had three source arrays firing every 16.6 m in consecutive order.

Results and discussion

As is common with OBC data, we applied deblending in the common receiver domain. Figure 2 shows receiver gathers from the dual-source survey. Blending noise is generally orders of magnitude larger than underlying signal. This is clearly noted on P-component data. High frequency energy at far offsets is also aliased, compromising the effectiveness of modeling attempts. Small residual from modeling imperfections can still overwhelm the data. For the Vz component, the record is contaminated by low-frequency background noise resulting from shear waves. The wavefield is too complex to be modeled adequately. This complexity also hinders the application of blind impulsive denoising, as signal damage is likely to occur. By deploying our combined deblending method, we were able to effectively separate blending noise from genuine source signal. Deblended data appear virtually free from blending noise, and difference sections show no signal leakage. The NSR maps for these gathers demonstrate how the guided impulsive denoise selects areas where it needs to operate. Note that this was only applied to the residual signal from the modeling stage in order to preserve signal as much as possible.

For the triple-source survey (Figure 3), as blending fold increases, cross-talk contamination becomes more intense. The noise amplitude level far exceeds that of the underlying signal. Randomness of next-shot blending noise is also less obvious. This is notable on both the P and Vz components. Similar to the dual-source case, blending noise was reasonably removed with minimal signal damage.

Sorting the data to common shot domain allows us to QC the process from a different view. Deblending inadequacies and signal leakage are easier to spot in this domain, as they are both coherent. Figure 4 shows the P-component data of the more challenging case of the triple-source survey. Energy from the three sources is observable on the records.

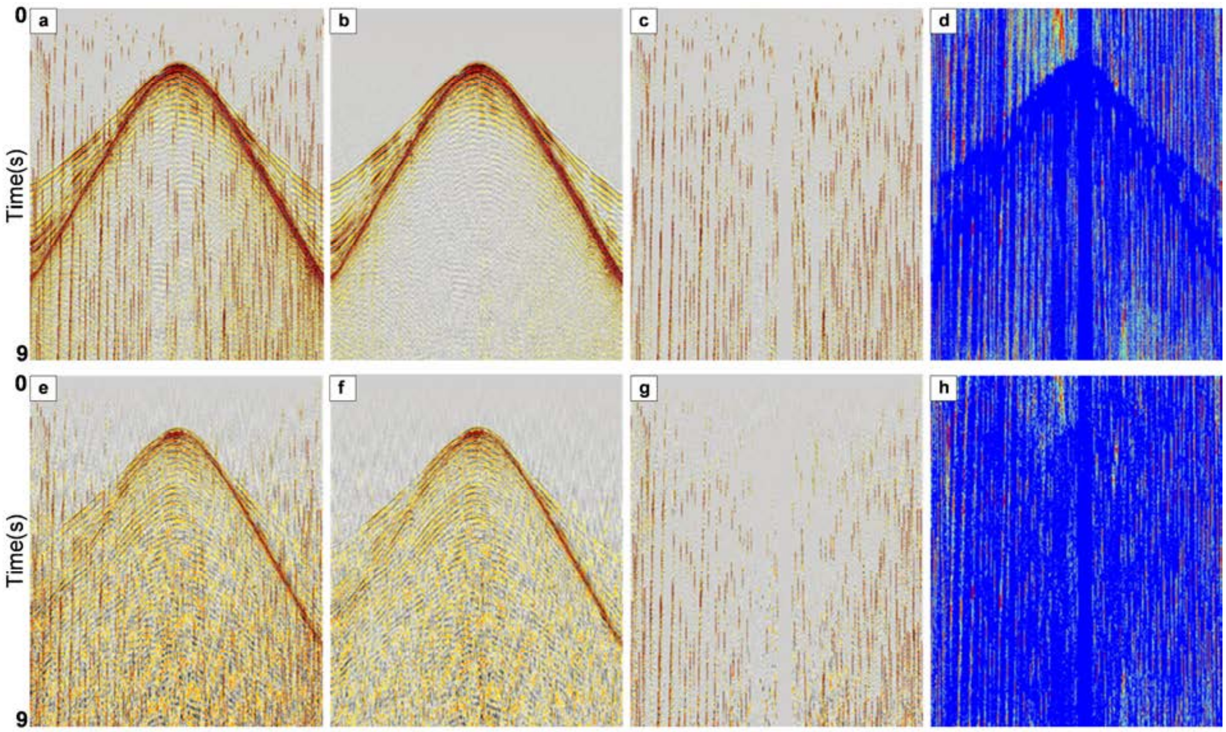

Figure 2. Common receiver gathers from the dual-source survey: P component (a) before deblending and (b) after deblending, with (c) difference and (d) corresponding NSR map; Vz component (e) before deblending and (f) after deblending, with (g) difference and (h) corresponding NSR map.

Relative amplitude differences between cross-talk and signal are also appreciable. Shot gathers confirm the previous observation that blending noise has been reasonably attenuated with minimal signal damage.

Figure 5 shows the migrated P component of the dual-source data with and without deblending. Observations derived from section views and depth slices are consistent with previous assessments from receiver and shot gathers.

In this study, we experienced several factors that added to the deblending challenge. High blending fold (up to 6) amplifies small errors in signal retrieval as these are accumulated through the alignment operator. Inversion of the true signal becomes complicated as the problem is severely underdetermined. In our implementation, the NSR map highlighted these regions, and the divergence of the solution was controlled through impulsive denoising. However, the lack of modeling accuracy compromised signal preservation relative to other regions with lower blending fold.

Another issue is background noise; this can be deceptive to modeling operators and often interferes with the deblending process. These operators can only estimate predictable parts of the signal relying on the neighborhood of the data, the assumption being that signal-to-noise ratio is sufficient. As long as the amplitude level of the noise is within reasonable limits, this does not create problems and minor inadequacies are recovered through standard processing and the stacking power of imaging.

In this study, our methodology performed reasonably well in dealing with these issues. However, in some areas, we saw some weak interference of background noise with deblending in the Vz component of the triple-source case. We also observed occasional strong residuals where shot intervals between different sources on one boat became too regular, such that the signal coherency/noise randomness criterion was absent. Both of these issues constituted such a negligible amount of data that effects on the final image were practically non-existent.

Conclusions

We have presented the complexities and challenges of source separation for shallow water OBC data. We developed a deblending methodology to deal with these challenges. The effectiveness of the methodology was demonstrated on different subsets of the survey with dual- and triple- source acquisition configurations, including both P and Vz components.

Acknowledgments

We would like to thank CGG and BP for permission to publish this work.

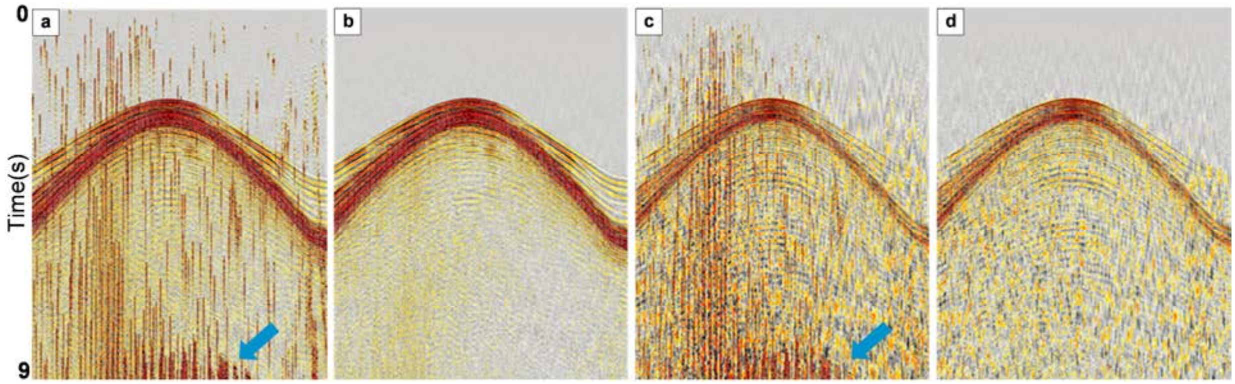

Figure 3. Common receiver gathers from the triple-source survey: P component (a) before and (b) after deblending; Vz component (c) before and (d) after deblending. (Arrows indicate the next shot blending noise.)

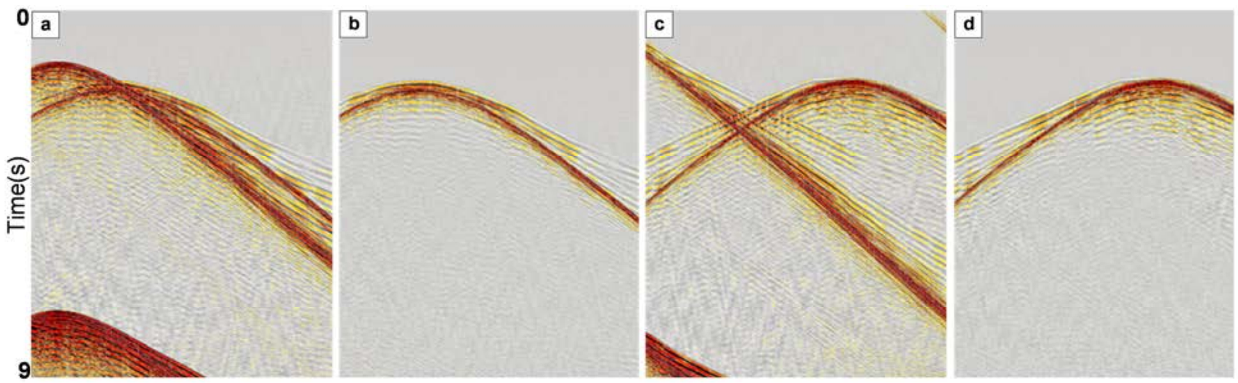

Figure 4. Common shot gathers from the triple-source survey: P component (a) before deblending and (b) after deblending; (c) before deblending and (d) after deblending.

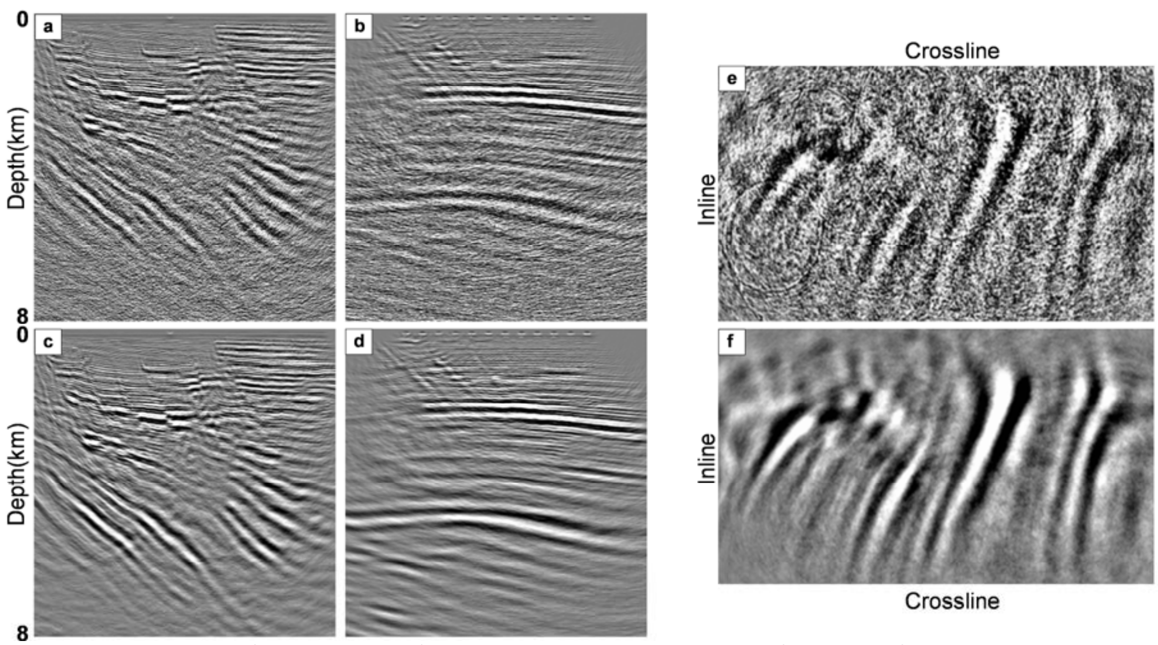

Figure 5. Migrated images of the P component from the dual-source survey: inline (a) before and (c) after deblending; crossline (b) before and (d) after deblending; depth slice at 5400 m (e) before and (f) after deblending.

REFERENCES

Abma, R., and J. Keggin, 2012, Simultaneous shooting, today and tomorrow: 74th Conference and Exhibition, EAGE, Extended Abstracts, workshop 03.

Abma, R., T. Manning, M. Tanis, J. Yu, and M. Foster, 2010, High quality separation of simultaneous sources by sparse inversion: 72nd Annual International Conference and Exhibition, EAGE, Extended Abstracts, B003.

Abma, R., Q. Zhang, A. Arogunmati, and G. Beaudoin, 2012, An overview of BP's Marine Independent Simultaneous Source Field Trials: 82nd Annual International Meeting, SEG, Extended Abstracts, 1-5.

Alexander, G., R. Abma, R. Clarke, SW. La Dart, M. Corzo, K. Gulette, J. Mika, and J. Kommedal, 2013, Processing results of simultaneous source surveys compared to conventional surveys: 83rd Annual International Meeting, SEG, Expanded Abstract, 104-108.

Howe, D., M. Foster, A. Allen, I. Jack, and B. Taylor, 2008, Independent simultaneous sources - a method to increase productivity of land seismic crews: 78th Annual International Meeting, SEG, Extended Abstract, 2826-2830.

Peng, C., and J. Meng, 2016, Inversion-based 3D deblending of towerd-streamer simultaneous source data using sparse Taup and wavelet transforms: 86th Annual International Meeting, SEG, Expanded Abstract, 4607-4611.

Rohnke, J., and G. Poole, 2016, Simultaneous source separation using an annihilation filter approach: 78th Annual International Conference and Exhibition, EAGE, Extended Abstracts, We LHR2 08.

Soubaras, R., 1995, Prestack random and impulsive noise attenuation by f-x projection filtering: 65th Annual International Meeting, SEG, Expanded Abstracts, 525-527.

Sternfels, R., G. Viguier, R. Gondoin, and D. Le Meur, 2015, Multidimensional simultaneous random plus erratic noise attenuation and interpolation for seismic data by joint low-rank and sparse inversion: Geophysics, **80**, no 6, WD129-WD141.

Wang, M., Z. H. Chen, C. Chen, F. C. Loh, T. Manning. S. Wolfarth, 2016, Advanced Deblending Scheme for Independent Simultaneous Source Data: 25th International Geophysical Conference and Exhibition, ASEG, Extended Abstracts, 564-568.